Supplemental Methods

Western blotting and ELISA

Tissues or cells were extracted in RIPA buffer supplemented with protease and phosphatase inhibitors (Roche, Complete Protease Inhibitor Cocktail, 04693116001 and Roche, PhosSTOP 049 06845001). Protein concentrations were determined using Pierce BCA Protein Assay (Thermo-Fisher, 23225). After boiling, 20-25 µg of protein was loaded onto 8% or 12% SDS – polyacrylamide gels. The membranes were then blocked with 5% milk in PBS and probed with primary antibody overnight at 4°C as follows: rabbit anti-pMLC2 S19 (Cell Signaling 3671), rabbit anti-MLC2 (Cell signaling 3672), goat anti-hVE-cadherin (R&D AF938), mouse anti- γ-tubulin (Sigma, T9026), or mouse anti- β-Actin (Sigma A5316). Membranes were then washed and incubated at room temp for one hour with light rocking in 5% milk and PBST with anti-species-specific secondary antibodies conjugated to LI-COR IRDye 680 or 800. Blots were washed in PBST and imaged on LI-COR Odyssey. The C3/C3a protein levels in the brain lysates were estimated using the mouse C3 ELISA kit (Genway, #GWB-7555C7) following the manufacturer's protocol.

Supplemental Figures and Figure Legends

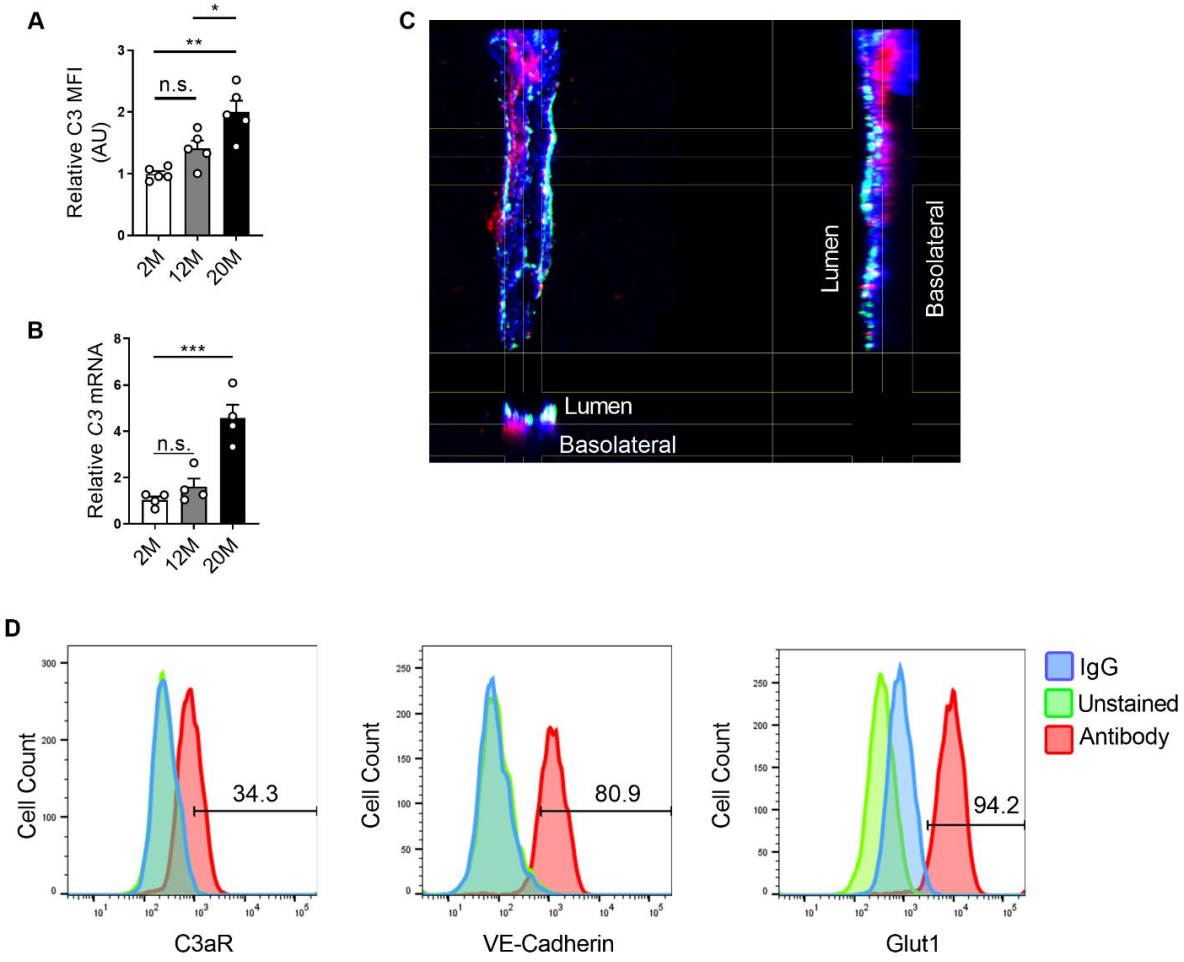

Supplemental Figure 1: Characterization of C3 and C3aR expression and localization. (A) Quantification of relative C3 mean fluorescence intensity (MFI) of images shown in Figure 1B. **(B)** qRT-PCR analysis of relative *C3* mRNA levels of FACS-sorted astrocytes. **(C)** High resolution orthogonal views of Glut1/C3aR/CD31 merged image in Figure 1E and IMARIS analysis of brain vessel showing expression of Glut1 (green) localized toward the lumenal surface and C3aR (red) localized toward the basolateral surface of a CD31 positive brain vessel. **(D)** Flow cytometry plots of HBMECs demonstrating highly expressed markers such as VE-Cadherin and Glut1 and lower but positive expression of C3aR. All significance was calculated using one-way ANOVA with Tukey's post hoc test (*p <.05, **p<.01, ***p<.001). n.s.: not significant.

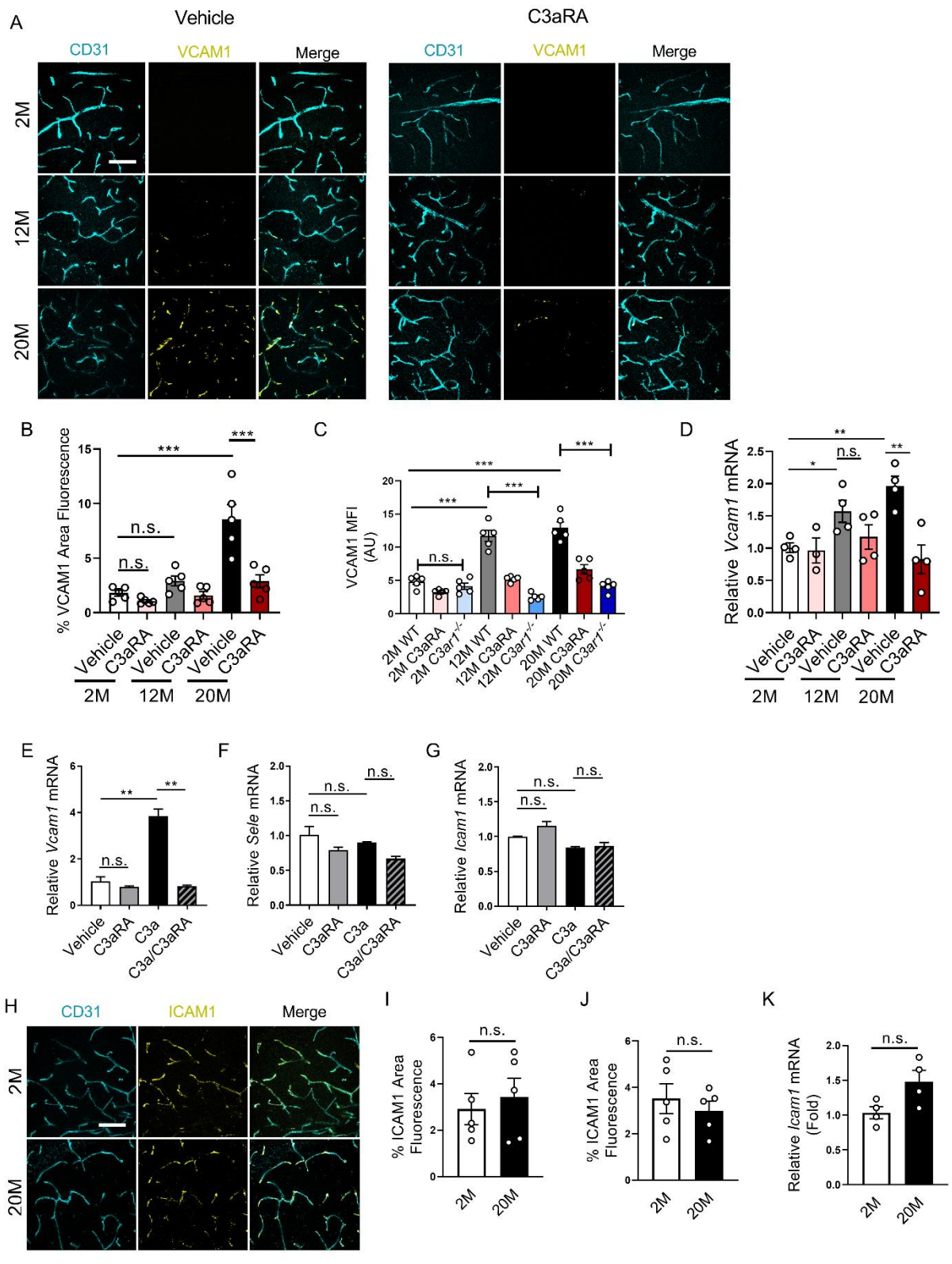
A
Vehicle
C3aRA
CD31
VCAM1
Merge
2M
12M
20M
B
% VCAM1 Area Fluorescence
n.s.
***
Vehicle
C3aRA
2M
12M
20M
C
VCAM1 MFI (AU)
2M WT
2M C3aRA
2M C3ar1-/-
12M WT
12M C3aRA
12M C3ar1-/-
20M WT
20M C3aRA
20M C3ar1-/-
D
Relative Vcam1 mRNA
*
**
E
Relative Vcam1 mRNA
Vehicle
C3aRA
C3a
C3a/C3aRA
F
Relative Sele mRNA
G
Relative Icam1 mRNA
H
CD31
ICAM1
Merge
I
% ICAM1 Area Fluorescence
J
% ICAM1 Area Fluorescence
K
Relative Icam1 mRNA (Fold)

Supplemental Figure 2: Elevated C3-C3aR signaling promotes VCAM1 expression in endothelial cells. (A, B) Mice treated with vehicle show increased VCAM1 expression with age, while C3aRA treated mice show similar reduction as the *C3ar1*$^{-/-}$ model in hippocampal endothelial cells at 20 months old. **(C)** Quantification of VCAM1 mean fluorescence intensity (MFI) in combined hippocampus and cortex demonstrates increased VCAM1 expression in WT aged brains and down-regulation by C3aRA or in *C3ar1*$^{-/-}$ mice. **(D)** qRT-PCR analysis of *Vcam1* mRNA expression of FACS-sorted brain endothelial cells from 2M, 12M, and 20M mice treated with vehicle or C3aRA for one month demonstrates the dependency on C3aR signaling. **(E)** Human brain microvascular endothelial cells treated with rhC3a increase *Vcam1* expression but did not increase expression of **(F)** *Sele* or **(G)** *Icam1,* and treatment with C3aRA was able to significantly reduce *Vcam1* expression. **(H)** Representative staining for ICAM1 and CD31 in 2M and 20M brain tissues. **(I and J)** Quantification of cortex (I) and hippocampus (J) demonstrating no change in ICAM1 fluorescence. **(K)** qRT-PCR analysis of sorted BECs showing no significant increase in aged brain *Icam1* gene expression. All data are means ± SEM of n = 4-5/group for all data plots. All significance was calculated using one-way ANOVA with Tukey's post hoc test, with the exception of (I), (J), and (K) which used two-tailed student's t-test (*p <.05, **p<.01, ***p<.001). n.s.: not significant. Scale bar = 50 µm.

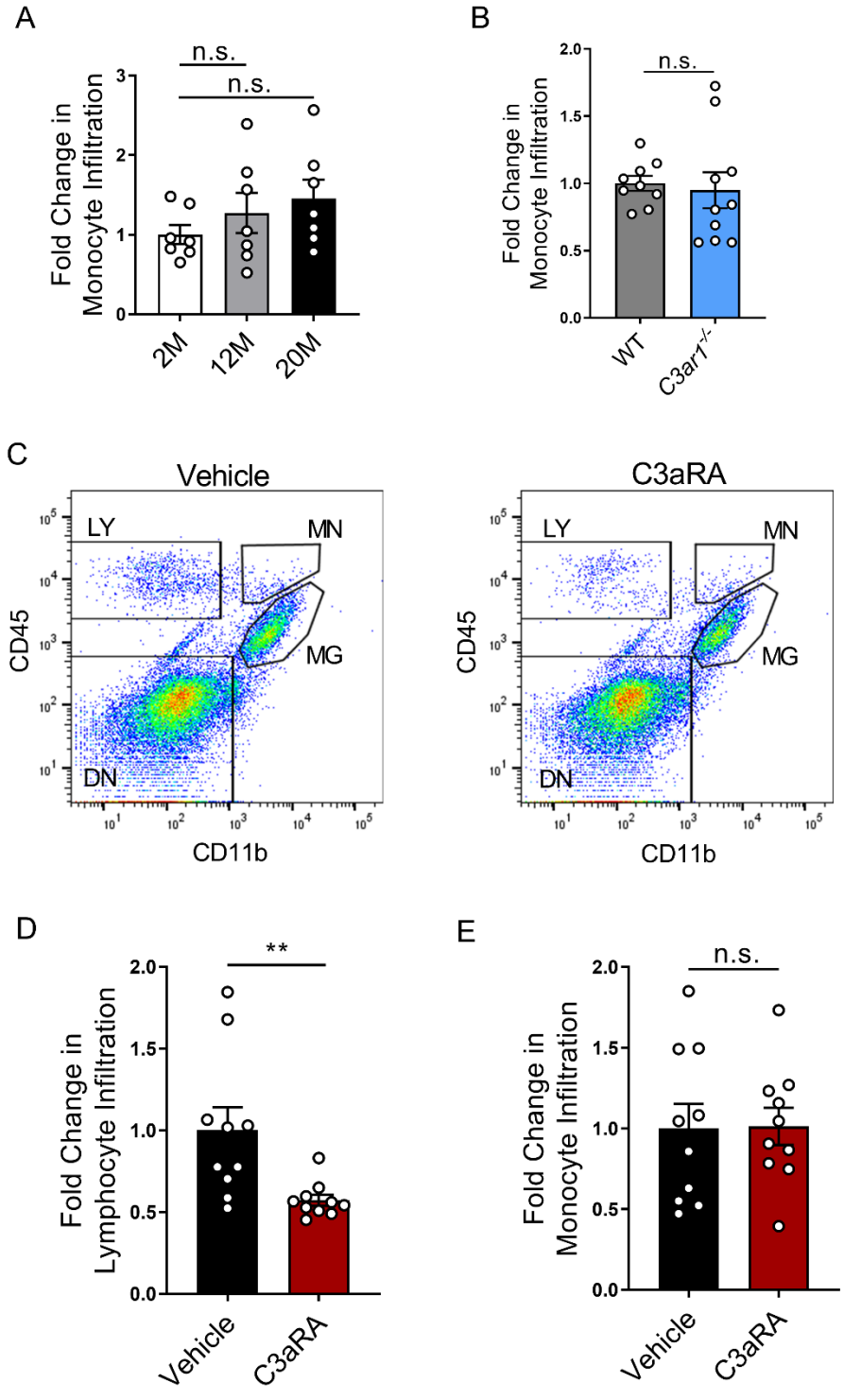
A
n.s.
n.s.
Fold Change in Monocyte Infiltration
2M
12M
20M
B
n.s.
Fold Change in Monocyte Infiltration
WT
C3ar1-/-
C
Vehicle
C3aRA
LY
MN
MG
DN
CD45
CD11b
D
**
Fold Change in Lymphocyte Infiltration
Vehicle
C3aRA
E
n.s.
Fold Change in Monocyte Infiltration
Vehicle
C3aRA

Supplemental Figure 3: Lymphocyte Infiltration is corrected by C3aRA treatment. (A, B) Monocyte number is not significantly increased in aged wild-type mouse brains or in 12-14-month-old wild-type vs. *C3ar1*$^{-/-}$ mouse brains. **(C-E)** Flow cytometry analysis of 20 month-old wild-type mice treated with vehicle or C3aRA (n = 10/group) show decreased lymphocyte infiltration but no change in monocyte numbers. All data are means ± SEM. Significance was calculated using one-way ANOVA with Tukey's post hoc test (A), or student's t-test (B, D, E) (*p <.05, **p<.01, ***p<.001). n.s.: not significant.

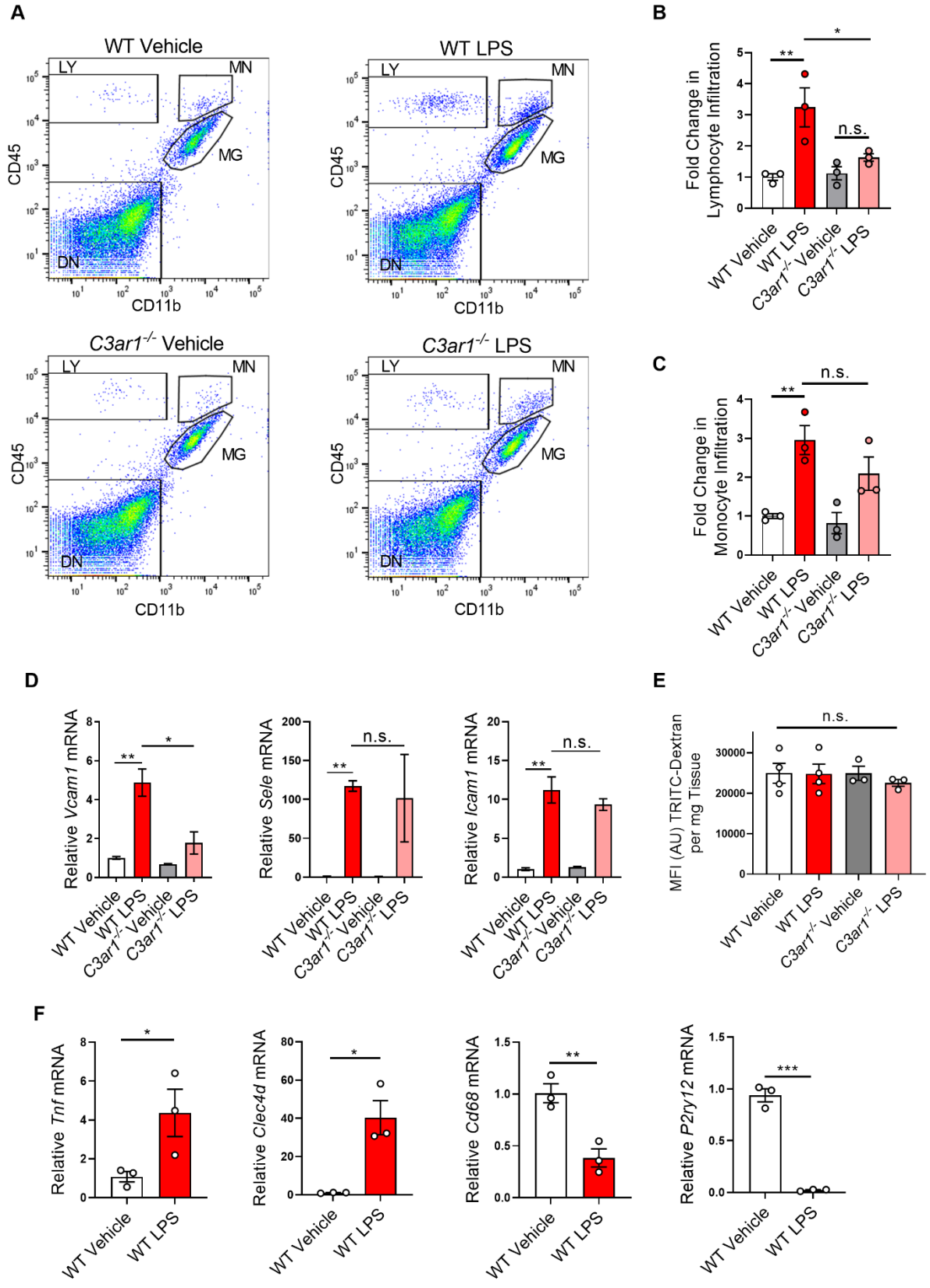
A
WT Vehicle
WT LPS
C3ar1-/- Vehicle
C3ar1-/- LPS
LY
MN
MG
DN
CD45
CD11b
B
Fold Change in Lymphocyte Infiltration
**
*
n.s.
WT Vehicle
WT LPS
C3ar1-/- Vehicle
C3ar1-/- LPS
C
Fold Change in Monocyte Infiltration
**
n.s.
D
Relative Vcam1 mRNA
Relative Sele mRNA
Relative Icam1 mRNA
E
MFI (AU) TRITC-Dextran per mg Tissue
n.s.
F
Relative Tnf mRNA
Relative Clec4d mRNA
Relative Cd68 mRNA
Relative P2ry12 mRNA
***

Supplemental Figure 4. Acute LPS stimulation affects lymphocyte infiltration in a C3aR-dependent manner. (A-C) Flow cytometry analysis of WT and *C3ar1*$^{-/-}$ mice challenged with dual i.c.v injection of vehicle or LPS for 24 hrs shows significant increases in lymphocyte and monocyte infiltration, but only lymphocyte infiltration is significantly rescued in *C3ar1*$^{-/-}$ mice. **(D)** 3-4-month-old wild-type mice challenged with LPS showed an increase in *Vcam1, Icam1,* and *Sele* expression in FACS-sorted brain endothelial cells analyzed by qRT-PCR, however, only *Vcam1* expression was rescued by *C3ar1*$^{-/-}$. **(E)** Blood-brain barrier assay using impenetrable TRITC-Dextran (65-85kDa) dye shows there is no permeability associated with acute neuroinflammatory response (n=3-4/group). **(F)** qRT-PCR analysis of microglia sorted from the vehicle and LPS injected animals demonstrates changes of microglia and neuroinflammatory signatures by LPS (n=3/group). All data are means ± SEM. All significance was calculated using one-way ANOVA with Tukey's post hoc test, with the exception of (F) which used two-tailed student's t-test (*p <.05, **p<.01, ***p<.001). n.s.: not significant.

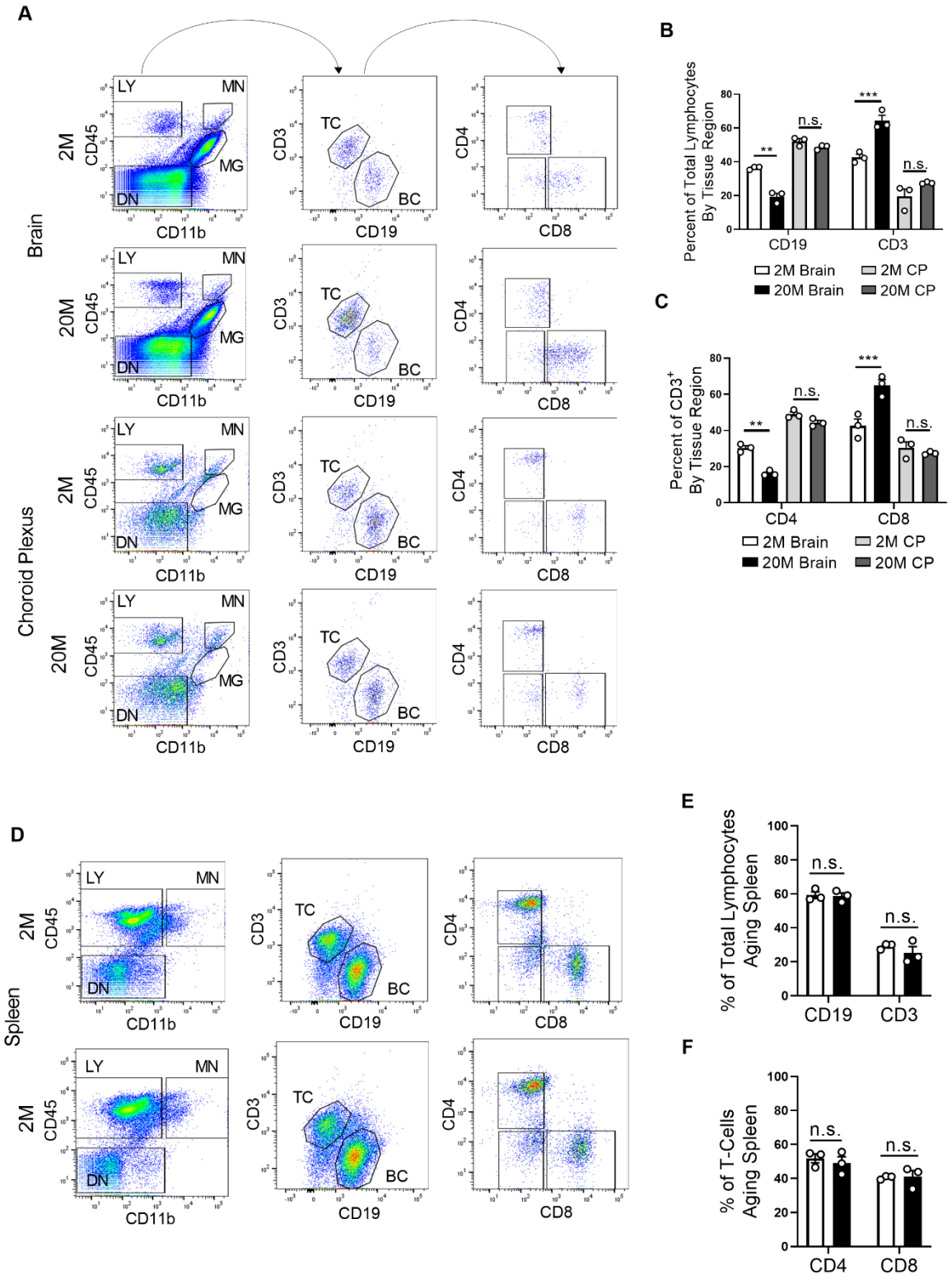
A
Brain
Choroid Plexus
2M
20M
CD45
CD11b
LY
MN
MG
DN
CD3
CD19
TC
BC
CD4
CD8
B
Percent of Total Lymphocytes By Tissue Region
CD19
CD3
2M Brain
20M Brain
2M CP
20M CP
n.s.
**
***
C
Percent of CD3+ By Tissue Region
CD4
CD8
D
Spleen
E
% of Total Lymphocytes Aging Spleen
F
% of T-Cells Aging Spleen

Supplementary Figure 5. Flow cytometry analysis of young and old brain, choroid plexus and spleen. (A) Schematic of flow cytometry analysis of dissociated 2M and 20M brain tissue compared to matched, resected choroid plexuses. **(B)** Quantification of the 2-month-old brain tissue compared with 20-month-old brain tissue shows increased $CD3^+$ T cell infiltration in the brain parenchyma, but no change in choroid plexus tissue in the aged brain. **(C)** Further flow cytometry analysis shows the subtype of T cell recruited is $CD8^+$ T cells with virtually no difference in cell type of the choroid plexus. **(D and E)** Representative flow data plots and quantification from aged spleen shows no change in T or B cell profiles with age, or changes in **(F)** CD4 and CD8 profiles. All data are means ± SEM of n = 3/group. Analysis was done using one-way ANOVA with Tukey's post hoc test (*p <.05, **p<.01, ***p<.001). n.s.: not significant.

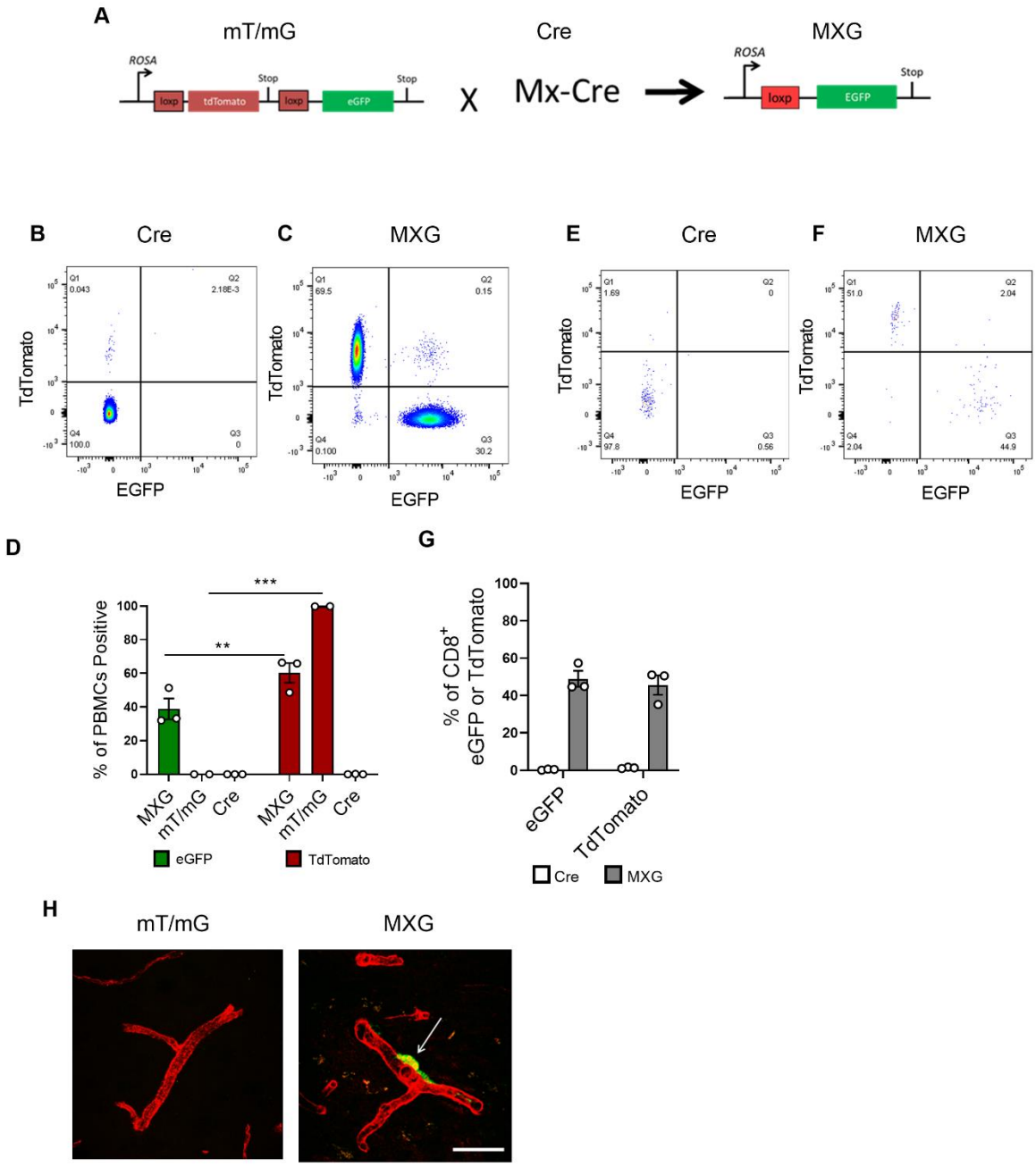
A
mT/mG
Cre
MXG
ROSA
loxp
tdTomato
Stop
loxp
eGFP
Stop
X
Mx-Cre
ROSA
loxp
EGFP
Stop
B
Cre
C
MXG
E
Cre
F
MXG
TdTomato
EGFP
Q1 0.043
Q2 2.18E-3
Q4 100.0
Q3 0
Q1 69.5
Q2 0.15
Q4 0.100
Q3 30.2
Q1 1.69
Q2 0
Q4 97.8
Q3 0.56
Q1 51.0
Q2 2.04
Q4 2.04
Q3 44.9
D
% of PBMCs Positive
***
**
MXG
mT/mG
Cre
MXG
mT/mG
Cre
eGFP
TdTomato
G
% of CD8+ eGFP or TdTomato
eGFP
TdTomato
Cre
MXG
H
mT/mG
MXG

Supplemental Figure 6. **MXG mice demonstrate immune cell infiltration along perivascular space. (A)** Schematic for genetics of MXG mouse model. **(B-D)** MXG mouse PBMCs expressing EGFP or TdTomato after recombination by Poly I:C induction. **(E-G)** Aged MXG mouse brains contain roughly equal proportions of EGFP and TdTomato expressing lymphocytes by flow cytometry. **(H)** Representative images of mT/mG mice and MXG mice showing EGFP expressing cells present along the perivascular surface of 15-month-old brain vasculature suggesting extravasation, infiltration, and perivascular residence. Scale bar = 20 μm.

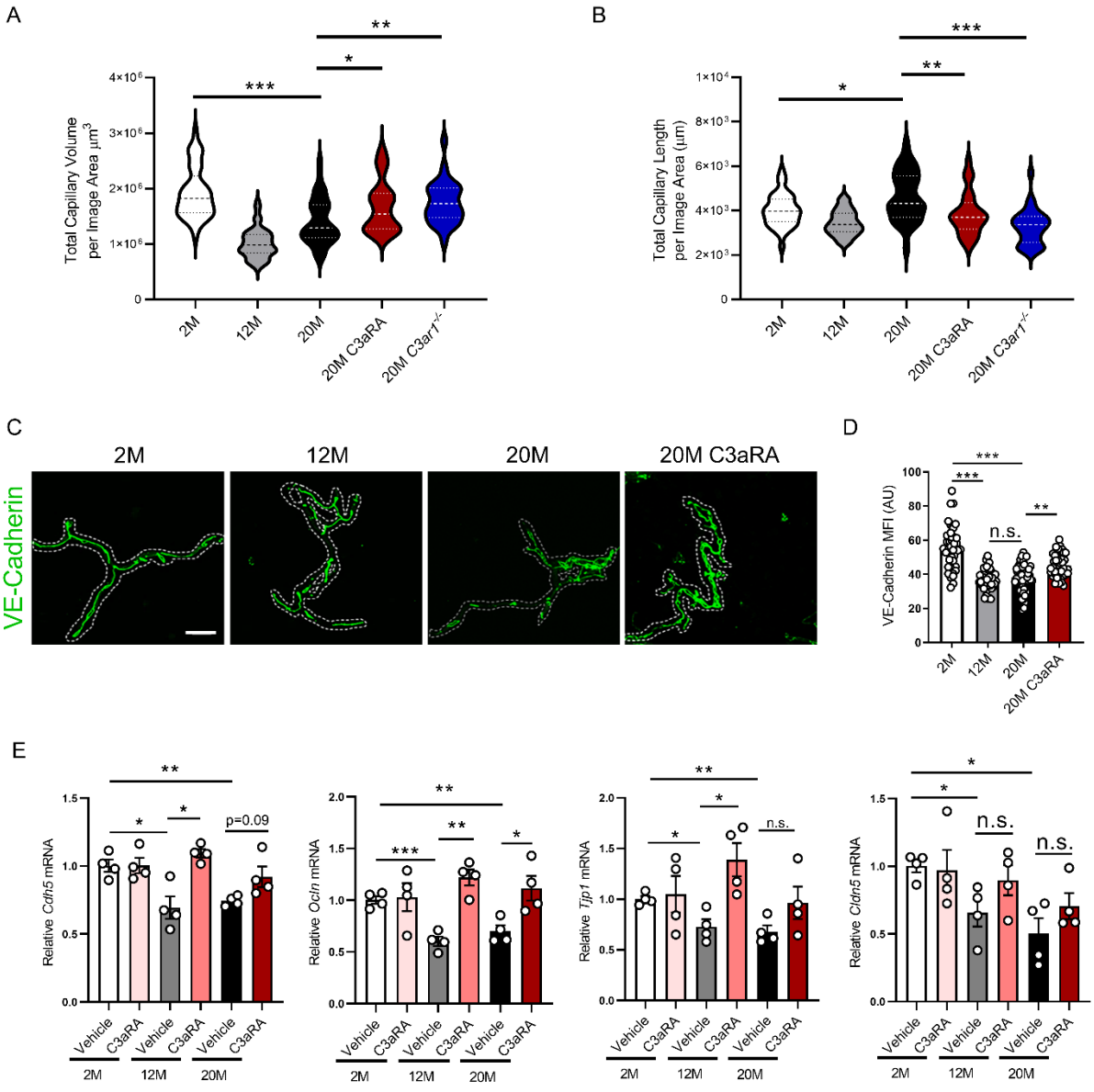
A
Total Capillary Volume per Image Area µm3
4×10^6
3×10^6
2×10^6
1×10^6
0
***
*
**
2M
12M
20M
20M C3aRA
20M C3ar1-/-
B
Total Capillary Length per Image Area (µm)
1×10^4
8×10^3
6×10^3
4×10^3
2×10^3
0
*
**
***
2M
12M
20M
20M C3aRA
20M C3ar1-/-
C
2M
12M
20M
20M C3aRA
VE-Cadherin
D
VE-Cadherin MFI (AU)
100
80
60
40
20
0
***
***
n.s.
**
2M
12M
20M
20M C3aRA
E
Relative Cdh5 mRNA
Relative Ocln mRNA
Relative Tjp1 mRNA
Relative Cldn5 mRNA
1.5
1.0
0.5
0.0
2.0
1.5
1.0
0.5
0.0
**
*
*
p=0.09
***
**
*
n.s.
Vehicle
C3aRA
2M
12M
20M

Supplemental Figure 7. C3aR activation alters vessel morphology and reduces expression of BBB associated genes. (A, B) Quantification of individual vessel dimensions measured for average-cross sectional area calculation shows that vessels decease overall volume with age and increase vessel length with advanced age. **(C)** Representative image of capillaries isolated from 2M and 12M mice or 20M mice treated with vehicle or C3aRA and stained with anti-VE-Cadherin. **(D)** Quantification of VE-Cadherin staining shows reduced VE-Cadherin expression in 12M and 20M mice, which is partially rescued in 20M mice treated with C3aRA (n=5/group, 5 vessel fragments/mouse). **(E)** qRT-PCR analysis of *Cdh5*, *Ocln*, *Tjp1* and *Cldn5* mRNA from FACS-sorted endothelial cells of 2M, 12M and 20M mice treated with vehicle or C3aRA (n=4/group). All data are means ± SEM. Statistical analysis was performed using one-way ANOVA with Tukey's post hoc test (*p <.05, **p<.01, ***p<.001). Scale bar = 10 μm. n.s.: not significant.

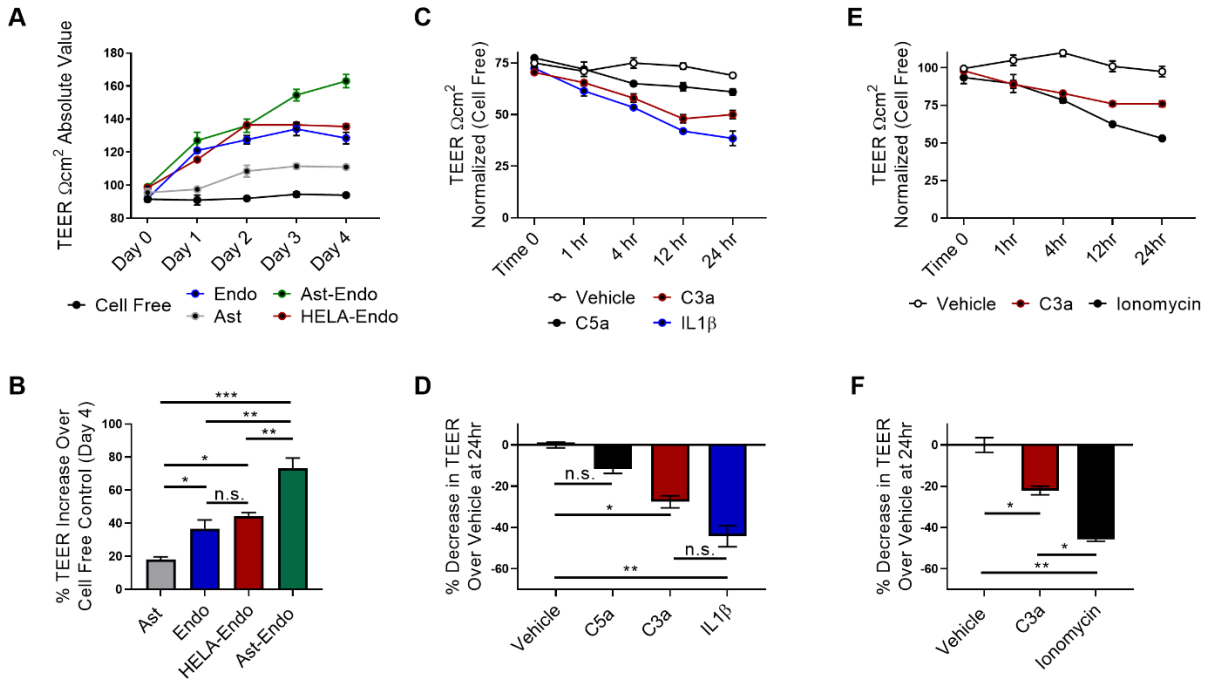

Supplemental Figure 8. C3aR activation induces Ca^{2+} mediated BBB permeability in TEER assay. (A, B) Validation of the co-culture system to develop a high-fidelity TEER for modeling the BBB. **(C, D)** Treatment of the system with C3a and IL-1β substantially reduces TEER compared to another complement family member C5a. **(E, F)** TEER values in co-cultures treated with vehicle, C3a or ionomycin over 24 hrs. All experiments were performed two independent times with each in duplicate and normalized to time-point control wells of cell free membranes. All data are means ± SEM and analysis was performed on average percent decrease in TEER using one-way ANOVA with Tukey's post hoc test (*p <.05, **p<.01, ***p<.001). n.s.: not significant.

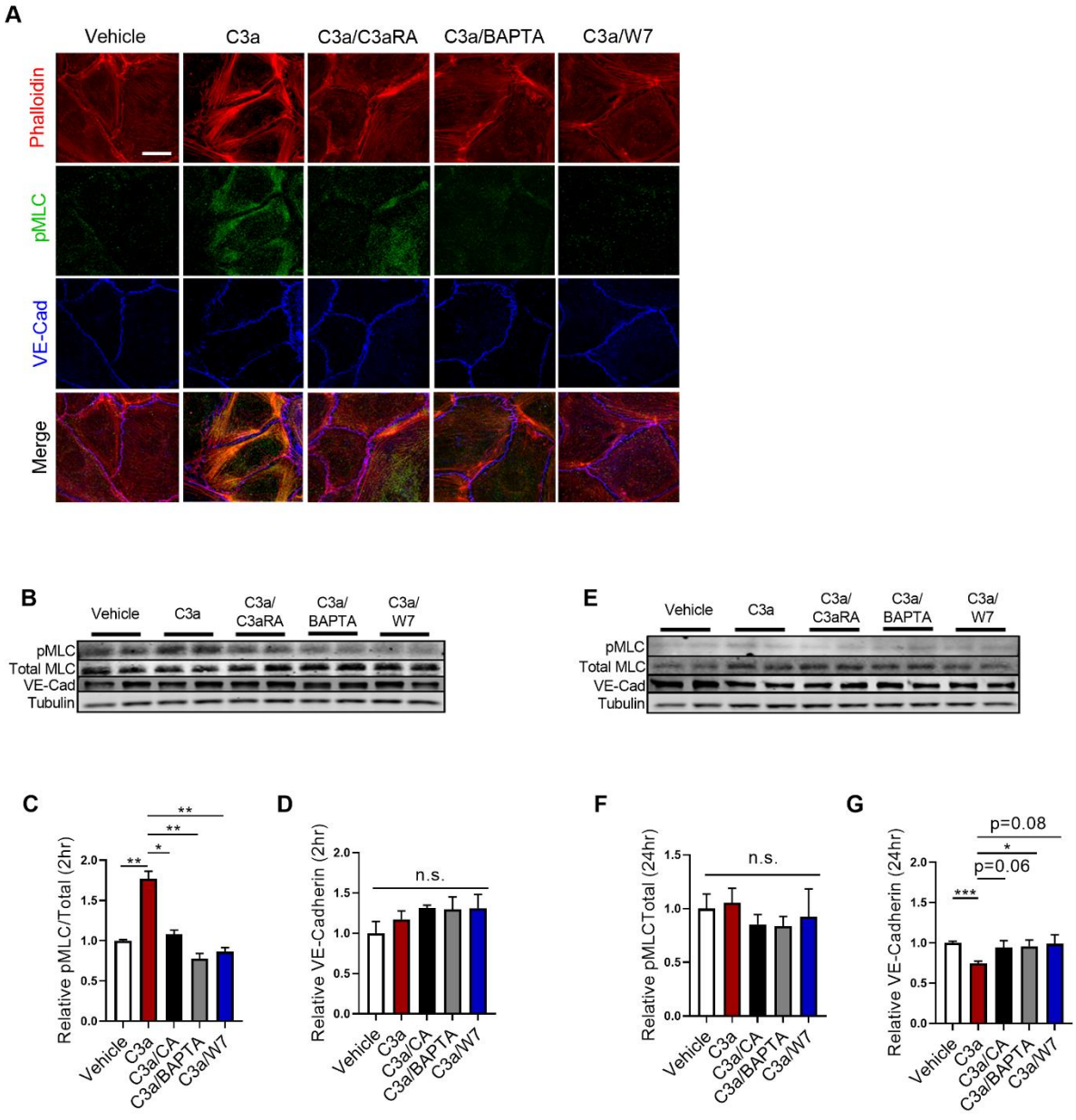
A
Vehicle
C3a
C3a/C3aRA
C3a/BAPTA
C3a/W7
Phalloidin
pMLC
VE-Cad
Merge
B
Vehicle
C3a
C3a/ C3aRA
C3a/ BAPTA
C3a/ W7
pMLC
Total MLC
VE-Cad
Tubulin
E
Vehicle
C3a
C3a/ C3aRA
C3a/ BAPTA
C3a/ W7
pMLC
Total MLC
VE-Cad
Tubulin
C
Relative pMLC/Total (2hr)
**
**
**
*
Vehicle
C3a
C3a/CA
C3a/BAPTA
C3a/W7
D
Relative VE-Cadherin (2hr)
n.s.
Vehicle
C3a
C3a/CA
C3a/BAPTA
C3a/W7
F
Relative pMLCTotal (24hr)
n.s.
Vehicle
C3a
C3a/CA
C3a/BAPTA
C3a/W7
G
Relative VE-Cadherin (24hr)
p=0.08
*
p=0.06
***
Vehicle
C3a
C3a/CA
C3a/BAPTA
C3a/W7

Supplemental Figure 9. C3aR activation induces Ca^{2+} release and stress fiber formation affecting BBB permeability. (A) Presence of increased F-actin (Phalloidin positive) stress fibers present in C3a treated HBMECs, rescued by blocking C3aR activation. **(B)** Representative Western blots of pMLC, total MLC, VE-Cadherin, and tubulin control. **(C, D)** Quantification of pMLC/total MLC and VE-Cadherin/tubulin shows increased pMLC which can be rescued by blocking Ca^{2+}, but no change in VE-Cadherin at 2 hrs (n=4/condition). **(E)** Representative Western blots of pMLC, total MLC, VE-Cadherin, and tubulin control. **(F, G)** Quantification pMLC/total MLC and VE-Cadherin/tubulin shows a normalized pMLC level with a decreased VE-Cadherin protein level which can be rescued by blocking Ca^{2+} signaling (n=4/condition). All data are means ± SEM. Analysis was performed using one-way ANOVA with Tukey's post hoc test (*p <.05, **p<.01, ***p<.001). n.s.: not significant. Scale bar = 5 µm.

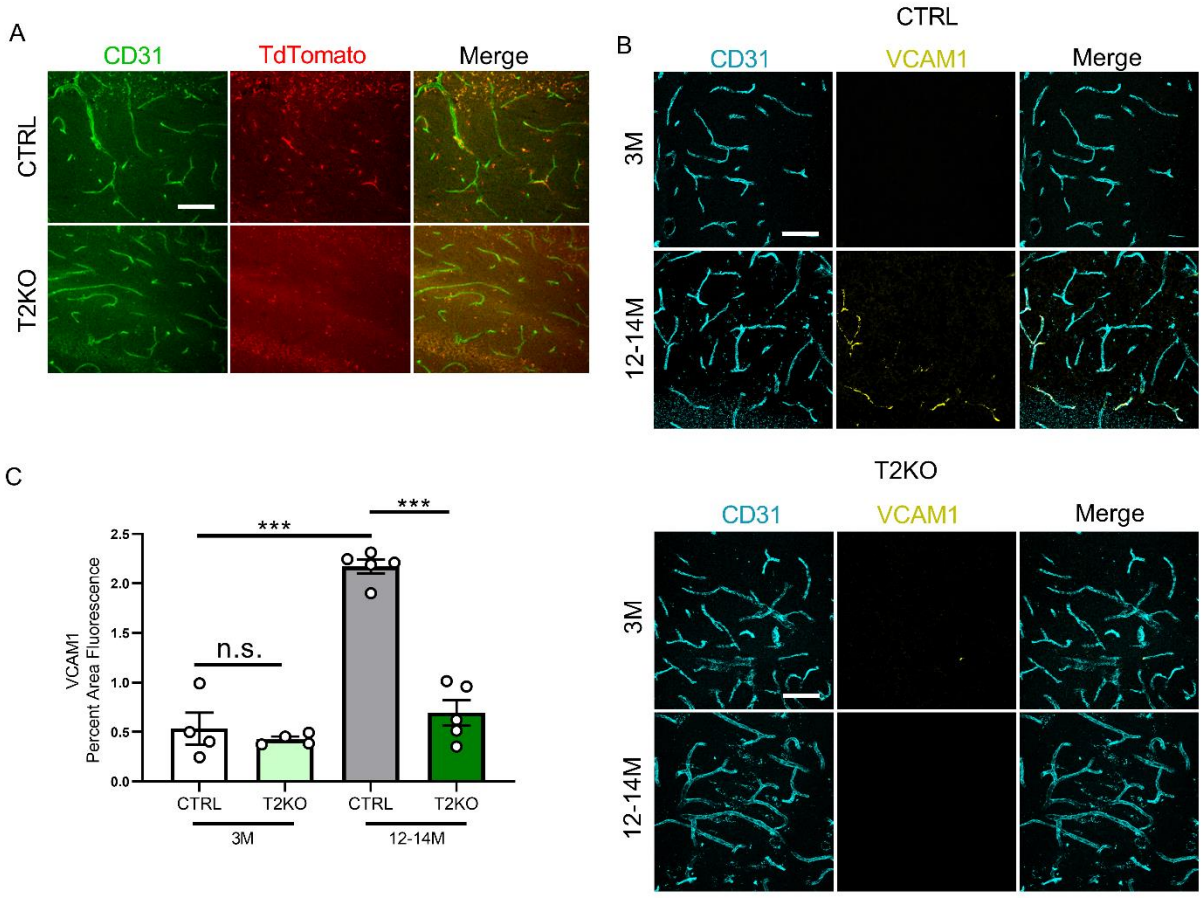

Supplemental Figure 10. Endothelial deletion of C3aR reduces age-related VCAM1 expression. (A) CD31 and TdTomato staining of *C3ar1* floxed-TdTomato reporter mice (CTRL) and with conditional deletion of *C3ar1* in endothelial cells (T2KO). **(B, C)** Analysis of VCAM1 expression in 3 and 12-14-month-old CTRL and T2KO mouse hippocampus demonstrates the rescue VCAM1 expression in T2KO. All data are means ± SEM. Analysis was performed using one-way ANOVA with Tukey's post hoc test (***p<.001). n.s.: not significant. Scale bar = 50 µm.

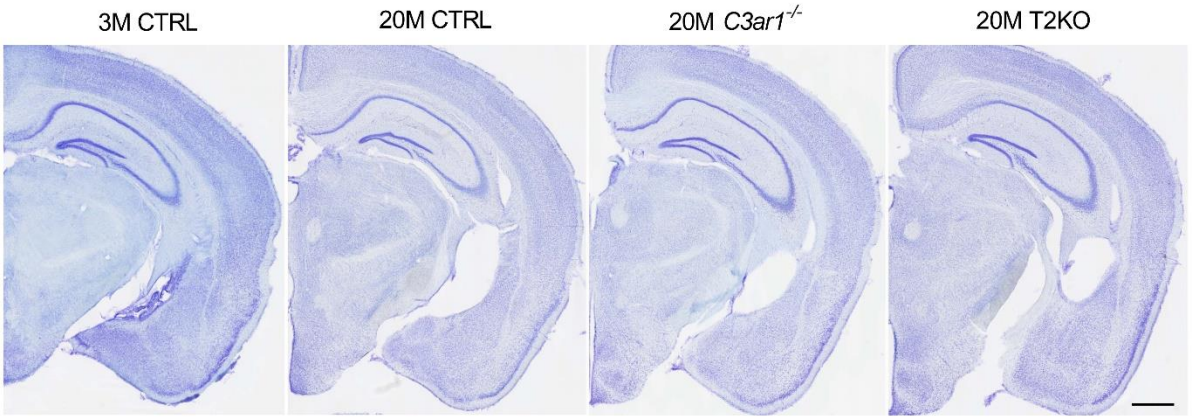

Supplemental Figure 11. Representative Nissl-stained hemi-brain images of young control (3M CTRL), aged control (20M CTRL), aged *C3ar1* null, or endothelial conditional knockout of *C3ar1* (T2KO). Scale bar = 700 μM.

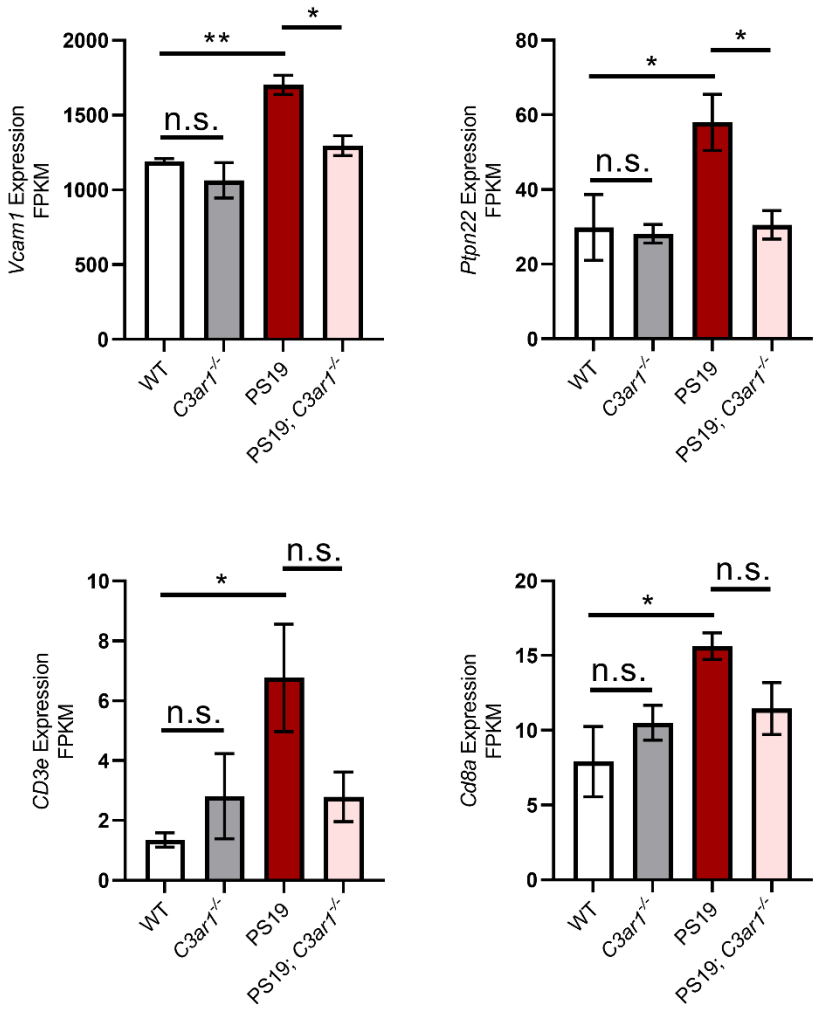

Supplemental Figure 12. RNA-seq data supporting C3aR-dependent CD8$^+$ T cell infiltration in PS19 mice. Increased expressions of *Vcam1, Ptpn22, CD3e* and *Cd8a* indicate the presence of CD3$^+$/CD8a$^+$ T cells in the hippocampus of PS19 mice, and a modest reduction in those expression signatures are observed in PS19;*C3ar1*$^{-/-}$ mice. All data are means ± SEM. Analysis for all results was performed using one-way ANOVA with Tukey's post hoc test (*p <.05, **p<.01, ***p<.001). n.s.: not significant.